FASTSAT-HSV01 THERMAL MATH MODEL CORRELATION

Callie McKelvey[1]
NASA Marshall Space Flight Center

Abstract

This paper summarizes the thermal math model correlation effort for the Fast Affordable Science and Technology SATellite (FASTSAT-HSV01), which was designed, built and tested by NASA's Marshall Space Flight Center (MSFC) and multiple partners. The satellite launched in November 2010 on a Minotaur IV rocket from the Kodiak Launch Complex in Kodiak, Alaska. It carried three Earth science experiments and two technology demonstrations into a low Earth circular orbit with an inclination of 72° and an altitude of 650 kilometers. The mission has been successful to date with science experiment activities still taking place daily. The thermal control system on this spacecraft was a passive design relying on thermo-optical properties and six heaters placed on specific components. Flight temperature data is being recorded every minute from the 48 Resistance Temperature Devices (RTDs) onboard the satellite structure and many of its avionics boxes. An effort has been made to correlate the thermal math model to the flight temperature data using Cullimore and Ring's Thermal Desktop and by obtaining Earth and Sun vector data from the Attitude Control System (ACS) team to create an "as-flown" orbit. Several model parameters were studied during this task to understand the spacecraft's sensitivity to these changes. Many "lessons learned" have been noted from this activity that will be directly applicable to future small satellite programs.

I. Introduction

The main purpose of the FASTSAT project was to minimize cost and schedule while generating a small (microsatellite) spacecraft market that provides opportunity for science, research and technology payloads of the NASA (National Aeronautics & Space Administration), DoD (Department of Defense), Intelligence and Aerospace Industry communities. FASTSAT-HSV01 kicked-off in January 2009 on an 11-month schedule from initial design to flight. Due to launch delays, the satellite flew 23 months after kick-off on a Minotaur IV rocket from the Kodiak Launch Complex in Kodiak, Alaska. It is typical for a project to correlate the design thermal math model to post thermal vacuum chamber and thermal balance testing results. This allows for a model correlation to a known set of environments in a controlled atmosphere. It also provides a test-correlated model to use during flight operations to assess any possible anomalies. However due to the nature of this project, the thermal balance test and post test model correlation effort was cancelled for schedule and funding reasons.

The FASTSAT-HSV01 "as-built" thermal math model was used to perform a correlation after launch with flight temperature data. This paper details that effort and is organized as follows:

---

[1]Aerospace Engineer, NASA Marshall Space Flight Center, Spacecraft & Vehicle Systems Department, Structural Design & Analysis Division, Thermal Analysis & Control Branch

Section II describes the thermal design of the satellite. Section III provides information regarding the flight data sets used for the correlation. Section IV outlines the approach for the correlation effort and presents the results from multiple trades considered to understand the spacecraft's sensitivity to varying model parameters. Section V contains the findings from this study and recommendations for future small spacecraft design and analysis work.

II. Thermal Design

The FASTSAT-HSV01 satellite consists of a roughly cubical bus including three interior mounting shelves for science and subsystems components and an exterior observation platform for payload components. Mounted within the bus is a Poly Picosatellite Orbital Deployer (PPOD) that deployed the Nano-Sail D satellite early in the mission. Services are provided to four additional experiments that remain with the spacecraft. The bus includes body mounted solar arrays consisting of 23 "clips" mounted on four sides as well as an additional clip on both the top and bottom surfaces. The bus provides conditioned power, data services, communication and navigation knowledge to the experiments.

FASTSAT-HSV01 does not have a stand-alone thermal control system. The thermal control is mostly passive relying on structural elements and equipment layout. There are no separate radiators, although the solar panels are attached to the structure and act as radiators when faced away from the Sun. Internal components are cooled via radiation and conduction, and mostly have high emissivity exterior surfaces to facilitate the radiative heat transfer. Figure 1 shows an integrated exterior view of FASTSAT-HSV01. Internal views of the satellite are considered sensitive until the mission is completed.

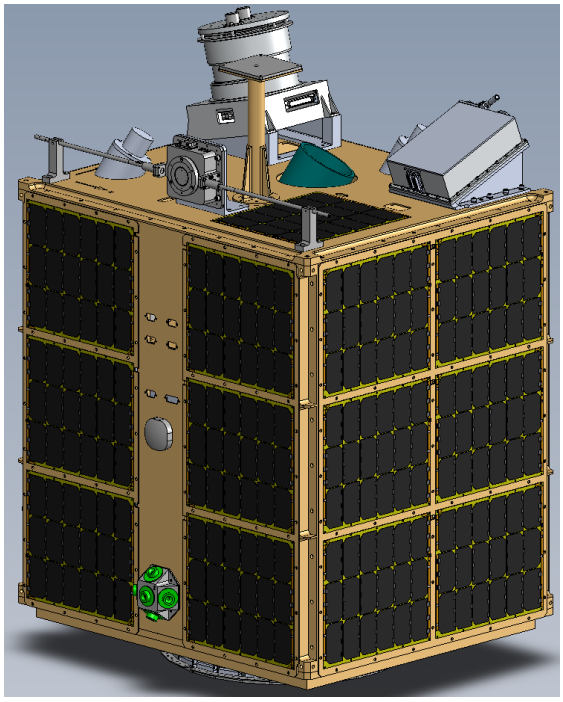

Figure 1. Integrated FASTSAT-HSV01

As previously stated, FASTSAT-HSV01 has 25 externally mounted solar clips. Each solar clip is comprised of 18 solar cells. The clips positioned on the four sides of the spacecraft as well as the single clip on the bottom side are mounted to thin aluminum plates. The top solar clip is mounted directly to the exterior observation platform. There are Resistance Temperature Devices (RTDs) mounted internally to the satellite on the aluminum plates centered behind each solar clip. These RTDs record representative temperatures for all 25 solar clips at one minute intervals throughout the life of the mission.

The thermal math model correlation was largely conducted using the 25 solar clip RTDs. Representative temperature "measures" were modeled within Thermal Desktop using the measures feature to assign an approximate location and average of the temperatures experienced in that specific location. Figure 2 shows the FASTSAT-HSV01 thermal model with the Thermal Desktop measures represented. Detailed temperature and power distribution telemetry for the internal instruments were not available for a full integrated correlation, but the intent of this activity was to verify a good thermal prediction of the primary structure, which serves as the primary thermal environment for any internally mounted instrument or payload.

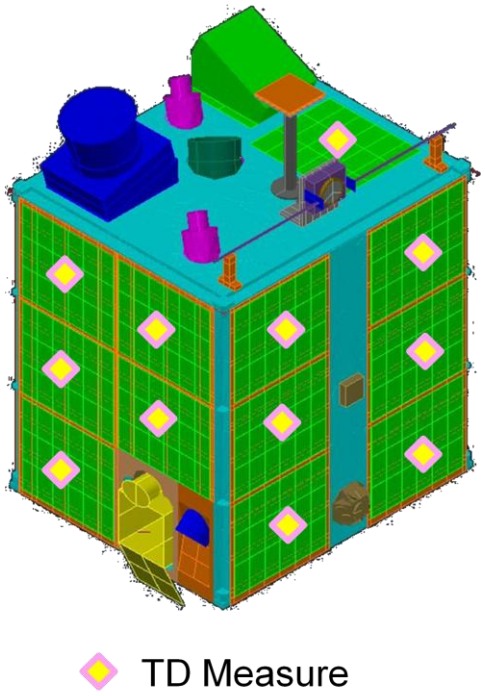

Figure 2. FASTSAT-HSV01 Thermal Math Model with RTDs/Thermal Desktop "Measures"

III. Flight Data Sets

The FASTSAT-HSV01 Attitude Control System(ACS) team provided actual Earth and Sun vector data, derived from onboard magnetometer and sun sensor readings, for two specific periods during the flight. The ACS data was recorded once per second for the duration of the mission. This information was easily imported into Cullimore and Ring's Thermal Desktop using the vector list orbit feature inside the Orbit Manager. The vector list orbit is defined by inputting a time, the vector to the Sun, the vector to the planet, and the ratio of the vehicle's distance from the planet center to the planet radius. The frequency of the flight ACS data was too detailed for the data sets used for the correlation effort. Therefore, the recorded flight ACS data was reduced to a position once every 5 minutes instead of once every second. This was considered a model parameter trade and is detailed further in Section IV.

The FASTSAT-HSV01 thermal math model has been correlated to two sets of flight data. The thought process behind selecting these data sets was to capture the following: 1.) Preferably 48 hours for each data set to allow plenty of time for the model to reach steady state conditions, 2.) one data set around beta angle 0° to represent a cold case, 3.) one data set around beta angle 75° to capture a hot case, 4.) no drop-outs in ACS data, 5.) preferably no drop-outs or very minimal losses in flight temperature recordings during the data set time period.

The first data set was taken on February 6, 2011. It was an 18 hour period around beta angle 0°. A longer period of data was requested, but due to a loss of signal only 18 hours of good data was available. The first orbit of this data set was run to quasi-steady state conditions, and was used to initialize the transient runs. A beta angle of roughly 0° was chosen because it represented several of the cold biased cases considered during the design and analysis phase. There were no losses of ACS data or temperature data during this 18 hour period. Data Set 1 is extremely unsteady as the spacecraft is rotating around the X, Y, and Z axis simultaneously.

Figure 3 shows a plot of the first data set averaged for each side. In an effort to simplify the graphs for this paper, most of the plots presented will show an average of the RTDs recordings for each side of the satellite. This allowed for six items per plot instead of twenty-five. The solar clips RTDs on each side of the spacecraft always trend together, so averaging the clips appeared to be an accurate representation of the actual mean temperatures. The correlation is conducted with averaged flight data therefore the averaged model data provides a direct comparison. Figure 4 shows all six solar clip RTDs on the +Y side individually as well as the average of the six RTDs. Section III shows a "one to one" plot with a direct RTD comparison with no averaging.

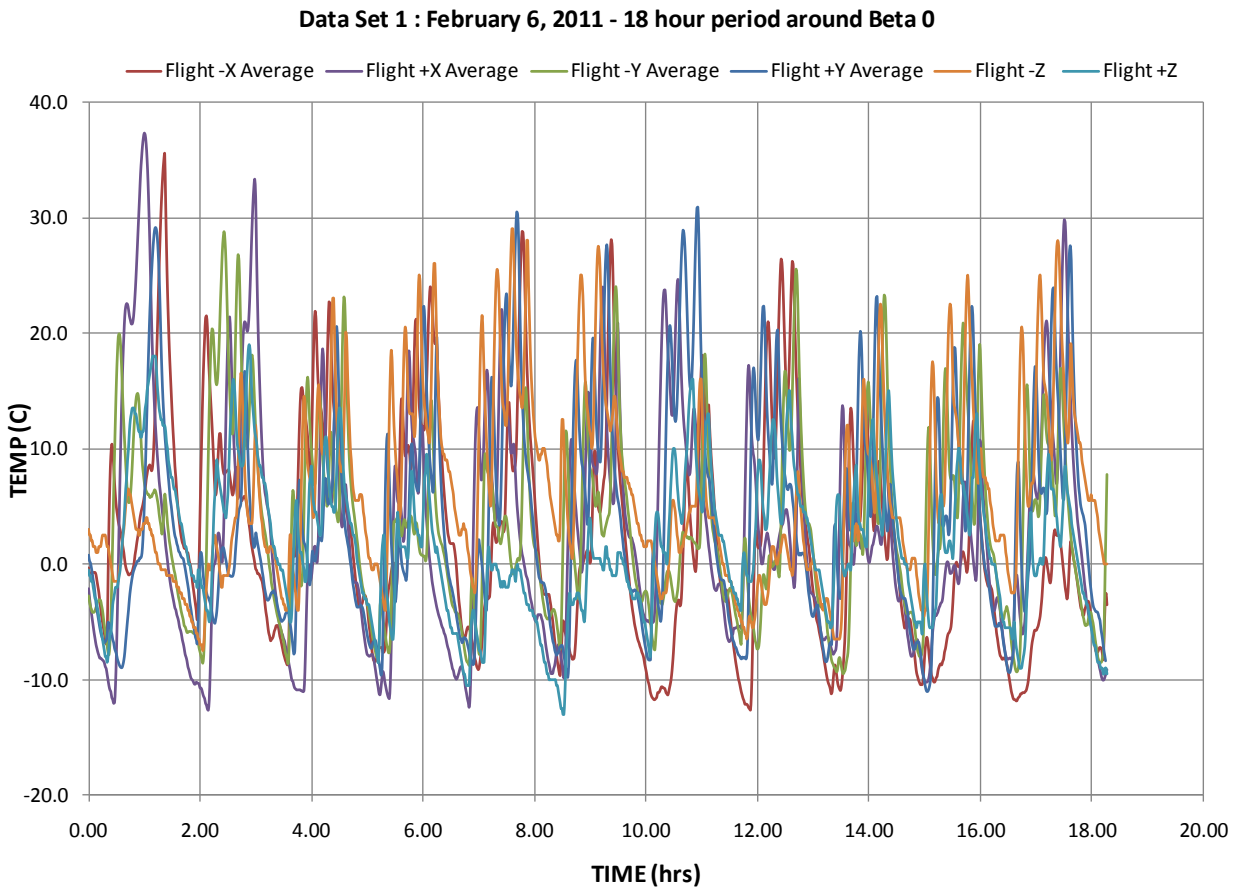

Figure 3. Data Set 1: February 6, 2011 - 18 hour period around Beta 0°

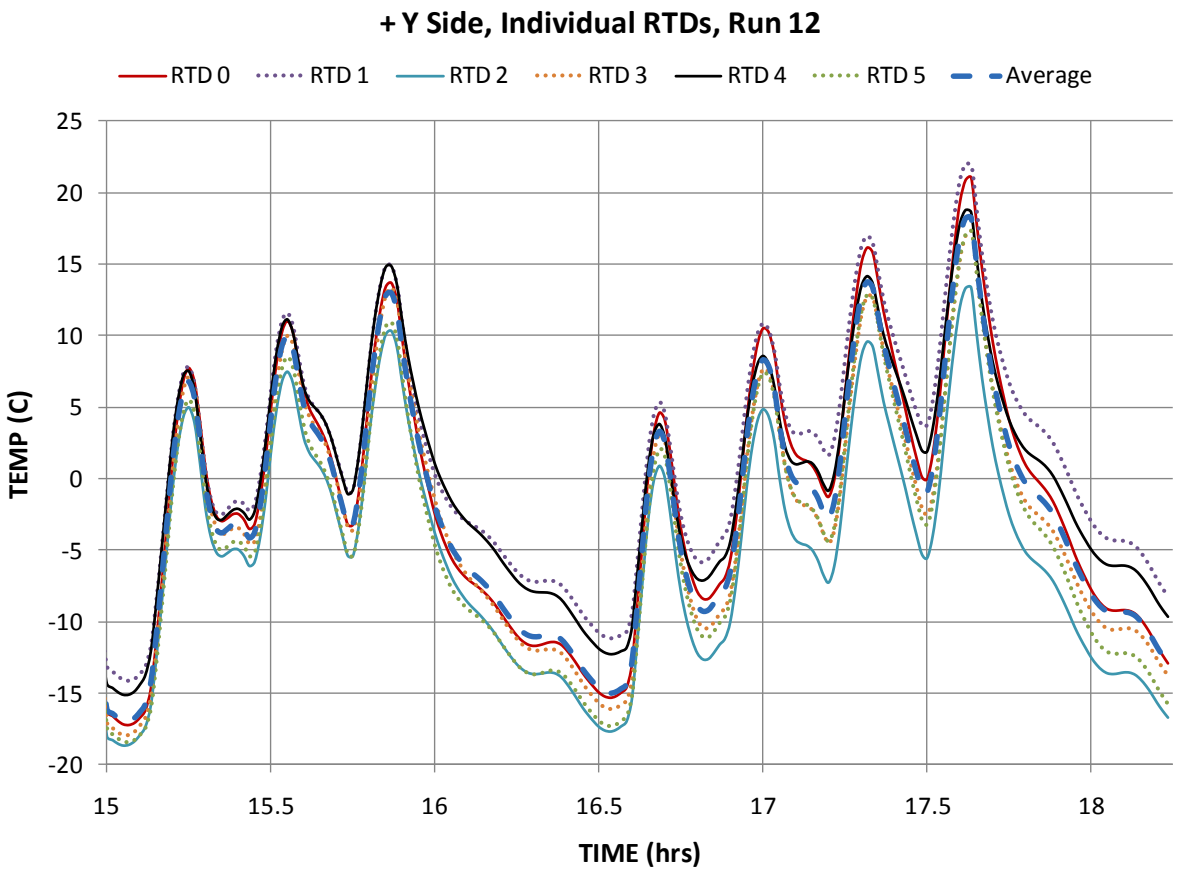

Figure 4. Data Set 1: +Y Side, all six RTDs plotted individually plus average of all six RTDs

The second data set was taken on March 11-12, 2011. It was a 48 hour period around beta angle 75°. A beta angle of roughly 75° was chosen because it is a full Sun orbit and represented several of the hot biased cases considered during the design and analysis phase. There were no losses of ACS data during this 48 hour period. However there was an almost five hour loss of flight temperature data. Since the ACS data was available during this period, it was possible to obtain estimated flight temperature data using the thermal model and the "as-flown" orbit data. Data Set 2 is still rather unsteady but the last 24 hours the +X side is always sun-facing and the -X side is always in shadow. Between the first and second data sets, the ACS team lost their magnetometer due to a sensor failure. One of the experiments housed a smaller magnetometer that the ACS team used to continue to capture pointing knowledge of the spacecraft. The flight ACS vector information for this data set had a few erroneous perturbations in the data. The best explanation for this is the transfer of control from the spacecraft magnetometer to the experiment magnetometer.

The flight temperatures external to the spacecraft ranged from 0C° to over +59°C during this recording period. The RTDs will only show temperature measurements of -68.5°C to +59°C. A restricted range was necessary due to maintain resolution, and this range was selected based on analysis data. During the hotter periods of the mission (around beta angle 75°), temperatures occasionally exceeded the +59°C capability. This can be seen in this second data set on the +X and +Y mounted solar clips.

Figure 5 shows a plot of the second data set. Similar to the plot shown in Figure 3, the RTDs on each side of the spacecraft have been averaged for simplicity in viewing the data.

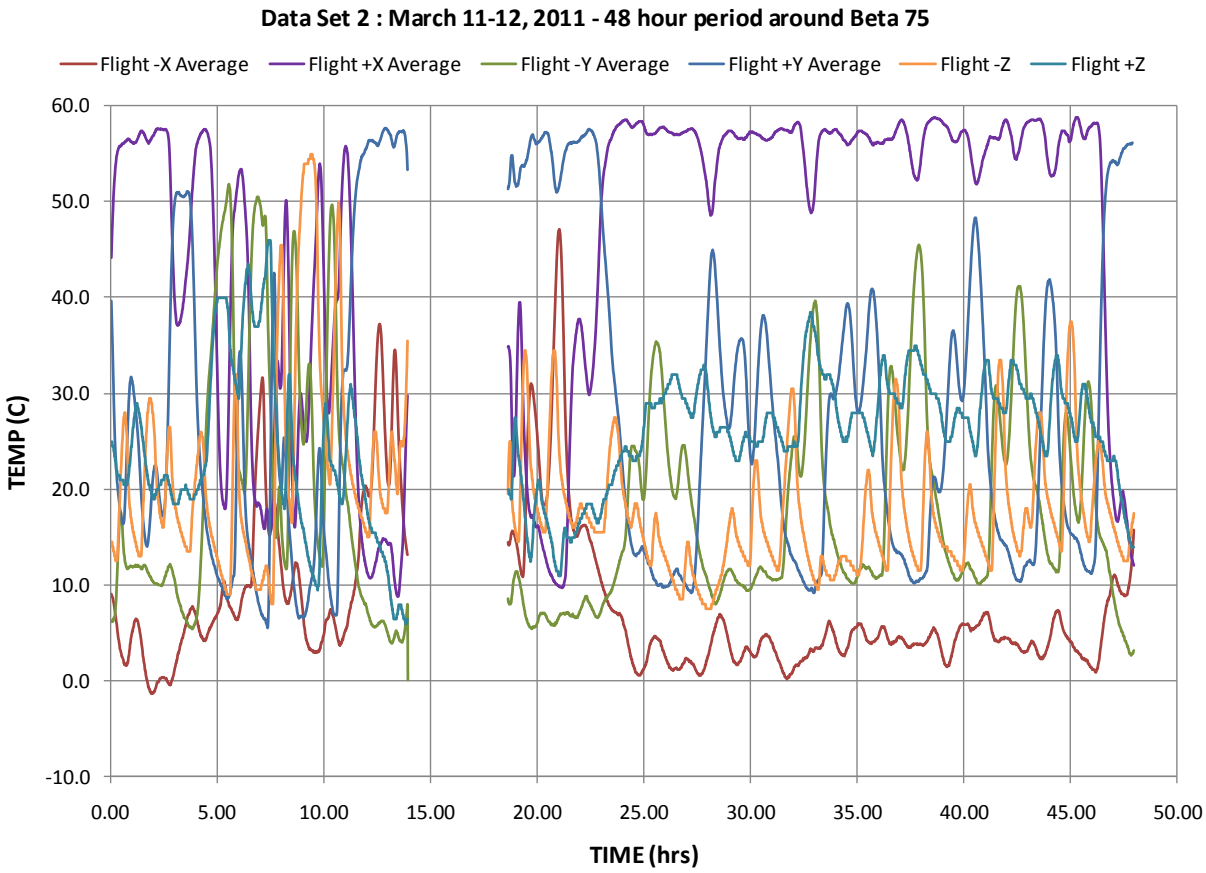

Figure 5. Data Set 2: March 11-12, 2011 - 48 hour period around Beta 75°

IV. Correlation Effort

A. Data Set 1 Correlation Summary

Twenty-eight cases were generated by varying model parameters in order to understand the spacecraft's sensitivity to these changes. Appendix A summarizes the details of each case study. All model runs were performed on a high-end workstation. The total run time for the model using the first data set was approximately 24 hours. The largest portion of this was the heating rate calculations which averaged around 18.5 hours to complete. Internal radiation calculations were fulfilled in a little over 4 hours, while external radiation calculations could be accomplished in less than 1 hour. The final SINDA run took a little over 30 minutes to complete.

As previously mentioned, the ACS vector data was supplied every second for this 18 hour data set. Using this much fidelity would have resulted in 64,800 orbital positions. At roughly 2 minutes of run time per position, it would have taken approximately 90 days to run.

This type of precision was not necessary to obtain an accurate correlation. Therefore, a position was pulled once every 5 minutes over the 18 hour data set. This resulted in a little over 200 positions. This proved to be a bit too coarse, thus the last two orbits provided an orbital position at 30 second intervals. The flight temperature data was correlated to the last two orbits of first data set.

Figures 6 and 7 show a comparison of flight data to analysis results, demonstrating the effects increasing the orbital position fidelity from every 5 minutes to every 30 seconds for the last two orbits. Figure 6 displays the average of all six solar clips on the +Y side, while Figure 7 shows the average of the six solar clips on the +X side. The solid blue line represents the flight temperature data. The dotted blue line displays the model temperatures from Run 1 which had an orbital position at 5 minute intervals. The solid green line represents Run 12 which had the increased fidelity to 30 second intervals for the final two orbits. Both Figures 6 and 7 are using the design thermal math model with only minimal parameter updates. These modifications will be detailed further on Page 13.

As shown in the following plots, increasing the position frequency provides a better correlation to the flight temperatures. The increased frequency brought out several peaks that were missed when using the 5 minute position intervals. The satellite was extremely unsteady during this 18 hour period causing the solar clip temperatures to vary greatly in short periods of time. This made it very important to increase the position occurrence for this data set to better capture the model predicted temperature profile.

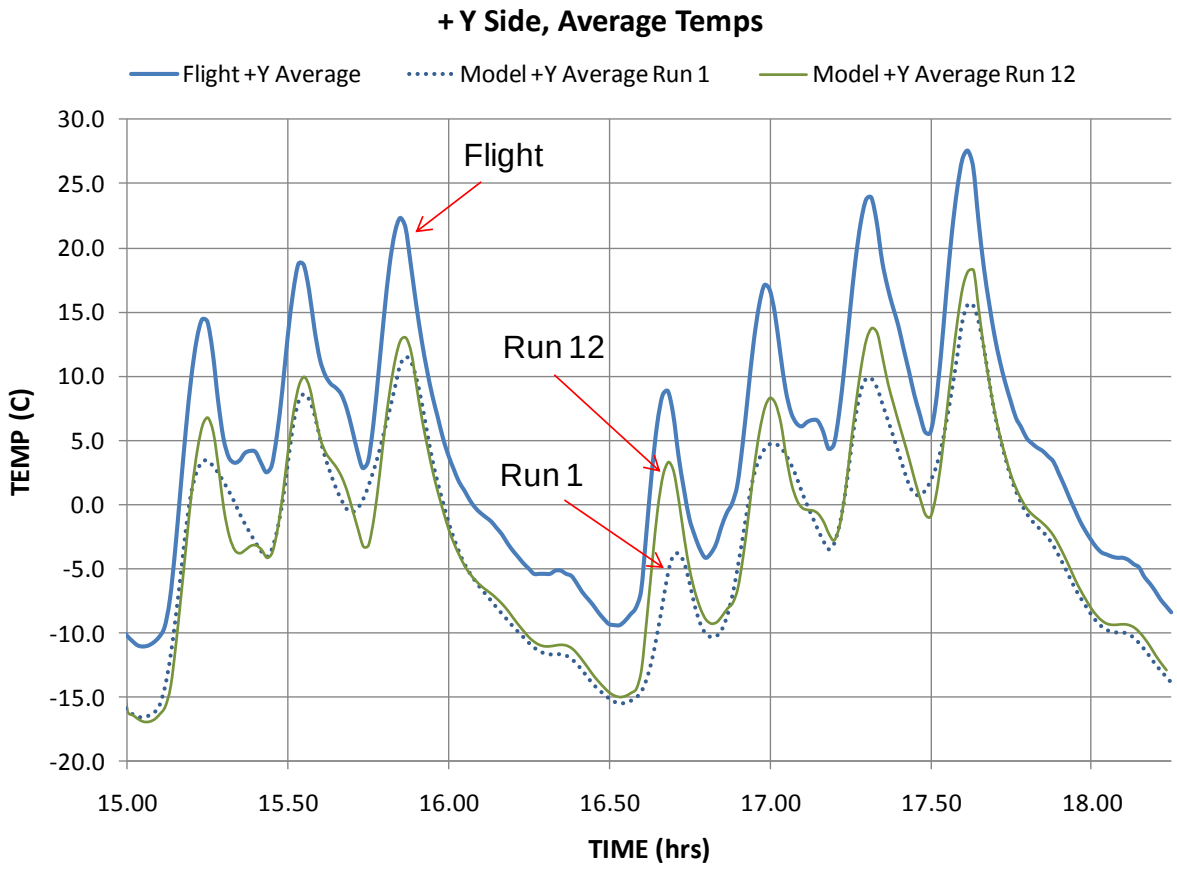

Figure 6. Data Set 1, +Y Side - Comparison of Orbital Position Frequency

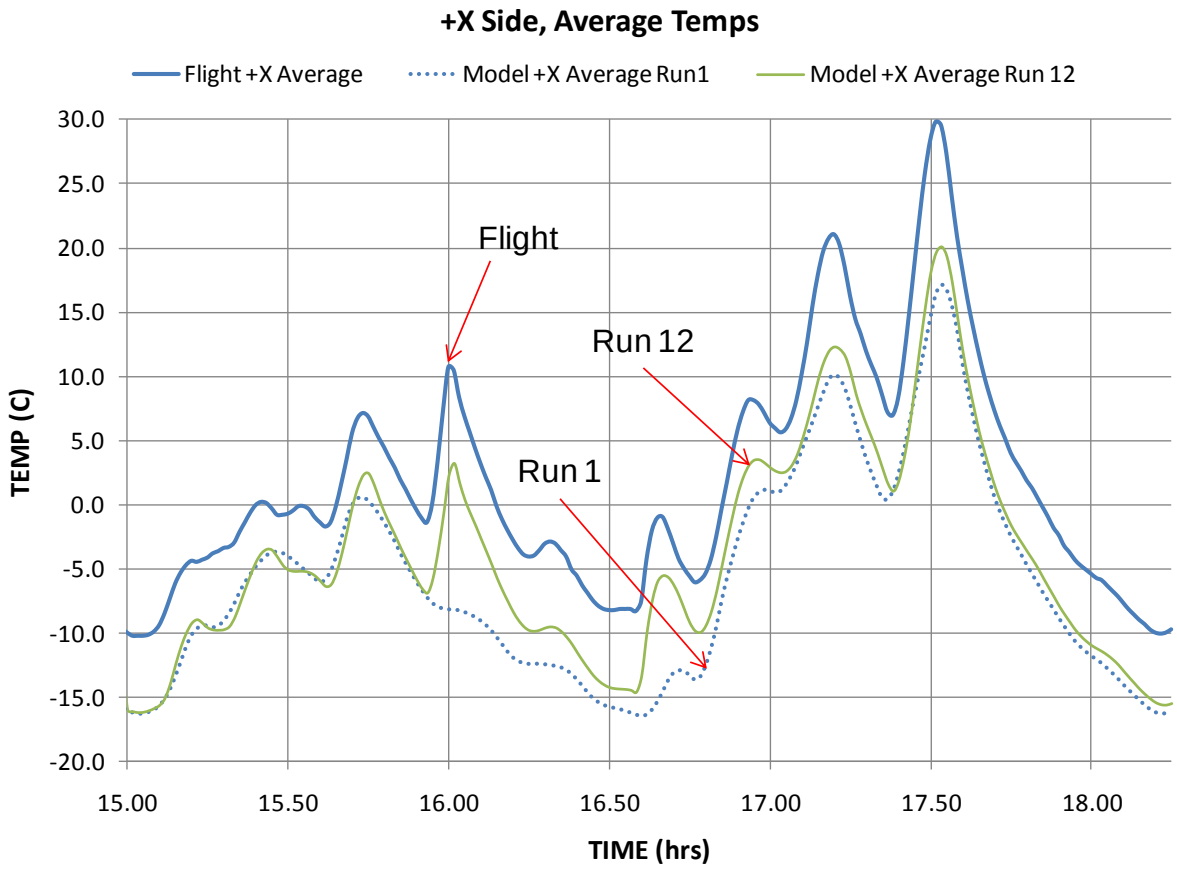

Figure 7. Data Set 1, +X Side - Comparison of Orbital Position Frequency

Figure 8 shows a "one to one" comparison of flight RTD 0 to model RTD 0, which is located on the +Y side. This plot also shows model average and flight average temperatures for the +Y side. It is shown using the results from the baseline case, Run 12, for the first data set. The solid red line represents RTD 0 model temperatures, while the dashed red line represents RTD 0 flight temperatures. The solid blue line represents model average temperatures for all six +Y RTDs, and the dashed blue line represents flight average temperatures for all six +Y RTDs.

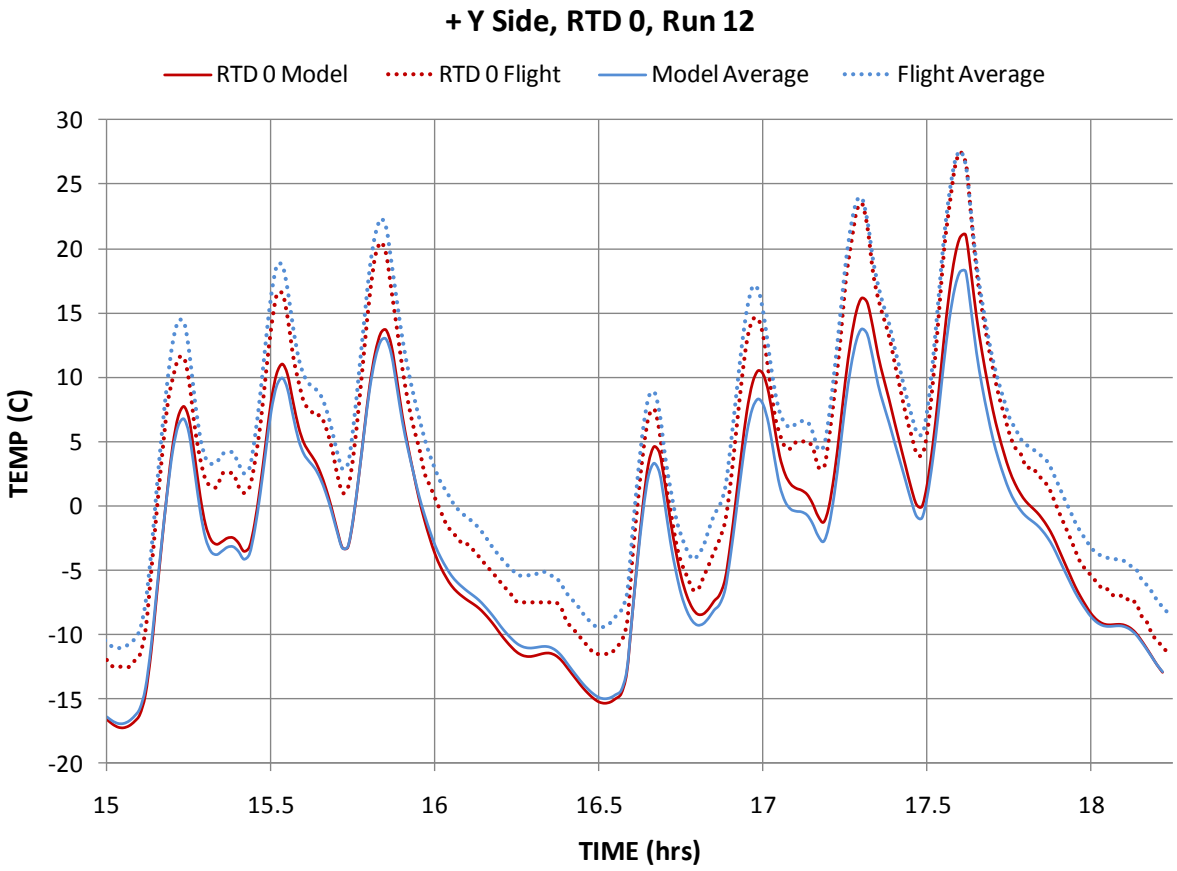

Figure 8. Data Set 1, +Y Side - "One to One" Comparison for RTD 0, Run 12

Only minimal changes were applied to the design phase thermal math model. The solar cell optical properties used during the design phase were for a silicon solar cell. The solar cells that were flown were GaAs (Gallium Arsenide) cells. The optical properties were modified to reflect the appropriate type of cell. The optical properties have a Sun angle dependent absorptivity based on the Kelly cosine factors and the efficiency of the solar cells. The following bullets and Figure 9 display those modifications.

- Design Data : $\varepsilon = 0.92$, $\alpha = 0.86$ (incorrect, silicon solar cell)
- Vendor Data : $\varepsilon = 0.85$, $\alpha = 0.92$ (correct, GaAs solar cell)
- Cell efficiency = 25.1%

Angle	apparent absorptivity
0	0.708
30	0.708
50	0.711
60	0.729
80	0.798
85	0.92
90	0.92

Figure 9. GaAs Solar Cell Sun Angle Dependent Absorptivity

The most uncertain part of this correlation effort is selecting the most appropriate set of external environments to apply. Because of the high inclination orbit, the majority of the Earth's surface is traversed during the mission, guaranteeing that a broad range of albedo and OLR (Outgoing Longwave Radiation) values are possible. Since FASTSAT-HSV01 does not include any sensors capable of determining external environments, NASA/TM-2001-211221[2] was referenced to obtain the mean expected environments on the satellite. A solar flux value of 1406 W/m^2 was calculated by scaling the median solar constant to the spacecraft's distance from the Sun on February 6, 2011. A mean albedo of 0.23 plus a 0.04 orbital average albedo correction factor was applied based on beta angle to give a total albedo value of 0.27. The mean OLR for high inclination orbits of 211 W/m^2 was also applied. Figure 10 shows a table from NASA/TM-2001-211221 where the environments above were defined. The mean values that were used are enclosed in green. The minimum albedo and OLR values are enclosed in blue, while the maximum values are enclosed in red. This information is highlighted to show the range of external environments that is possible for this correlation. Figure 11 displays the albedo correction factor recommendations from NASA/TM-2001-211221. The correction factor of 0.04 was applied to the first data set to represent a beta angle of 0°, while a correction factor of 0.19 was applied to the second data set for a beta angle of 75°.

[2] Guidelines for the Selection of Near-Earth Thermal Environment Parameters for Spacecraft Design, B.J. Anderson-Marshall Space Flight Center, C.G. Justus & G.W.Batts - Computer Sciences Corporation of Huntsville, Alabama

Table 4.2.3-3. Engineering Extreme Cases for High Inclination Orbits

Albedo and OLR values are referenced to the "top of the atmosphere", R_E + 30 km.

	COLD CASES		
Averaging Time	**Minimum Albedo** Alb ⇔ OLR (W/m²)	**Combined Minimum** Alb ⇔ OLR (W/m²)	**Minimum OLR** Alb ⇔ OLR (W/m²)
16 second	0.06 ⇔ 273	0.16 ⇔ 212	0.40 ⇔ 108
128 second	0.06 ⇔ 273	0.16 ⇔ 212	0.38 ⇔ 111
896 second	0.09 ⇔ 264	0.17 ⇔ 218	0.33 ⇔ 148
30 minute	0.13 ⇔ 246	0.18 ⇔ 218	0.31 ⇔ 175
90 minute	0.16 ⇔ 231	0.19 ⇔ 218	0.26 ⇔ 193
6 hour	0.18 ⇔ 231	0.20 ⇔ 224	0.27 ⇔ 202
24 hour	0.18 ⇔ 231	0.20 ⇔ 224	0.24 ⇔ 205
	HOT CASES		
Averaging Time	**Maximum Albedo** Alb ⇔ OLR (W/m²)	**Combined Maximum** Alb ⇔ OLR (W/m²)	**Maximum OLR** Alb ⇔ OLR (W/m²)
16 second	0.50 ⇔ 180	0.32 ⇔ 263	0.22 ⇔ 332
128 second	0.49 ⇔ 184	0.31 ⇔ 262	0.22 ⇔ 331
896 second	0.35 ⇔ 202	0.28 ⇔ 259	0.20 ⇔ 294
30 minute	0.33 ⇔ 204	0.27 ⇔ 260	0.20 ⇔ 284
90 minute	0.28 ⇔ 214	0.26 ⇔ 244	0.22 ⇔ 250
6 hour	0.27 ⇔ 218	0.24 ⇔ 233	0.22 ⇔ 221*
24 hour	0.24 ⇔ 224	0.23 ⇔ 232	0.20 ⇔ 217*
Mean Albedo: 0.23		**Mean OLR:** 211	

* Dark side OLR data was included to reach these figures; thus they may underestimate the maximum to always-daylight sun synchronous satellites by perhaps 15 W/m².

Figure 10. External Environments for High Inclination Orbits

Table A-2 provides pulse-averaged SZA correction terms for albedo for pulses beginning at or symmetrical about solar noon. That is, the average was taken from solar noon to the time indicated, assuming a 90-minute circular orbit and using the method in STEM. As the numbers indicate, the correction term is not a strong function of orbit position because the average has been weighted with cos(SZA) in accordance with variation of albedo energy.

Table A-2. Pulse-averaged SZA Correction Terms for Albedo Assuming a 5400-s Orbit. Add the Indicated Correction to the Value for SZA = 0.

Beta Angle	Max Time From Solar Noon			
	128 s	448 s	896 s	1350s or More (Orbit Average)
0	0.01	0.02	0.03	0.04
10	0.01	0.02	0.03	0.04
20	0.02	0.02	0.04	0.05
30	0.03	0.03	0.04	0.06
40	0.04	0.04	0.05	0.07
50	0.05	0.06	0.07	0.09
60	0.08	0.09	0.10	0.12
70	0.13	0.13	0.15	0.16
80	0.20	0.21	0.22	0.22
90	0.31	0.31	0.31	0.31

Figure 11. Albedo Correction Factors based on Beta Angle

As seen in Figures 6 and 7, the first few runs of the first data set correlation effort proved to be fairly agreeable. The model temperatures trend nicely with the rise and fall of the flight temperature data. The model temperatures are running about 5-10°C cooler than the flight values. After reviewing the first set of runs, several model parameters were varied to better understand the spacecraft's sensitivity to these parameter trades and close the temperature gap between the flight temperatures and the model predictions.

Contact conductance values were the first consideration. The model contains a representative contactor between the aluminum panels (where the solar clips are mounted) and the satellite structure to characterize thermal coupling. This value was increased by a factor of 10 and also zeroed out to represent complete isolation of the aluminum panels. Although both of these changes had a significant effect on the model to flight temperature comparison neither effect closed the temperature gap. Increasing the contactor values tied the solar clips more closely to the thermal mass of the spacecraft thereby slowing the response time and "flattening" the model predicted temperature profile. Isolating the aluminum panels had the opposite effect as the temperature swings were more extreme on the hot and cold side and induced a quicker response time. Figure 12 shows the +Y side solar clips with the aluminum plate isolated from the spacecraft. Once again the solid blue line represents the flight temperature. The dotted blue line represents Run 12, which is the baseline case using the design contact conductance values. The dashed green line represents Run 24, which includes the isolation of the aluminum panels.

The contactors that represent the adhesive used to mount the solar clips to the aluminum panels were also varied widely with only minimal effect.

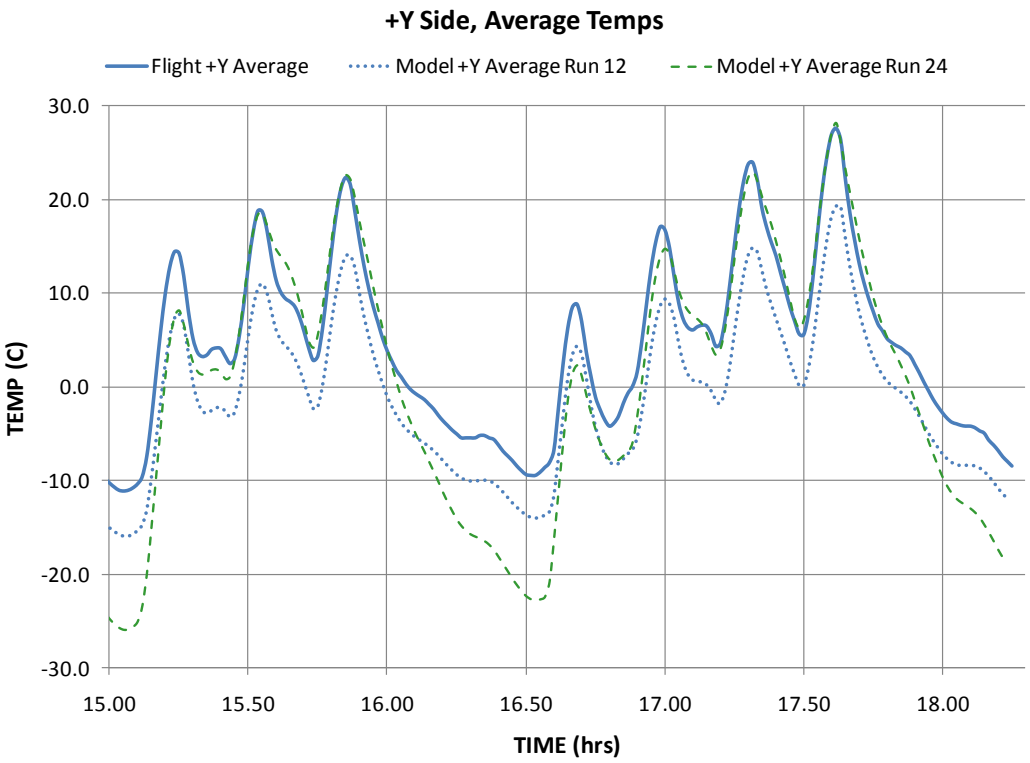

Figure 12. Result from varying model conductance values

Internal and external emissivity values were considered next. Most of the interior surfaces are black anodized aluminum. The design emissivity value was 0.90. A case was run with an emissivity value of 0.82 with very little effect on the model predicted temperatures of the solar clips. The externally mounted solar cells had a design emissivity of 0.85. Multiple cases were considered with the following emissivity values: 0.80, 0.75, and 0.70. The model predicted temperatures responded positively to changes in this parameter. Lowering the solar cell emissivity values increased the model predicted temperatures and would completely close the temperature gap when using an emissivity value of 0.70. Midway through the correlation effort, the optical properties were tested on a flight spare solar cell. This test resulted in absorptivity and emissivity values of α=0.925 and ε=0.83, which are very close to the vendor data values of α=0.92 and ε=0.85. After the optical properties test, the test values were applied to all future runs.

Convergence criteria factors were tightened and this resulted in zero effect on the model predicted temperatures.

The variation of the mentioned modeling assumptions either had very little effect on predicted temperatures or did not give the response needed for an improved correlation. Therefore, the temperature difference between flight data and analysis appears to be caused by difference between the assumed nominal external environment and the environment that was actually experienced during flight. The actual flight environment is probably some combination of higher albedo and OLR. As shown in Figure 10, 3σ values can be as high as 0.54 for albedo and 332

W/m^2 for OLR. While not likely that both values would be that high for a single orbit, one value could be high while the other might be closer to average.

Multiple cases were considered using average albedo values with extreme OLR values, and then using an average OLR value with a higher albedo value. Figures 13, 14, and 15 display the +Y and +X sides and the battery temperature comparisons of Run 12 versus Run 21. The RTD used for the battery comparison is located on the lid of the battery box internal to the spacecraft. Run 12 is the baseline case with the mean albedo and OLR values of 0.27 and 211 W/m^2 respectively. Run 21 shows a case with the mean albedo value of 0.27 and an extreme OLR value of 300 W/m^2.

As noticed in Figures 13, 14 and 15, the higher OLR value provides a nice correlation for the first data set. Although there is no way of knowing the exact external environments during this 18 hour period on February 6, 2011 it is probable that the OLR the satellite experienced during this period was higher than the mean.

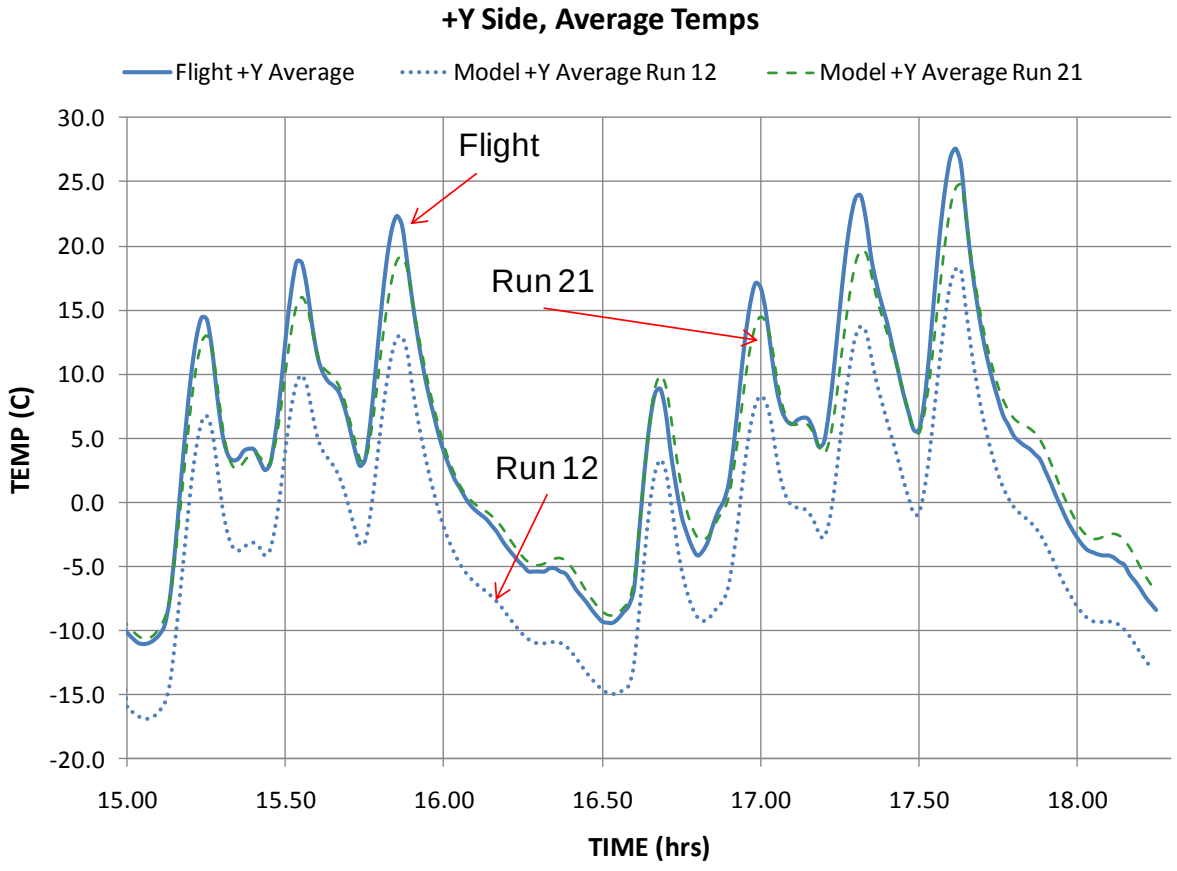

Figure 13. +Y Side - Result from increased OLR value

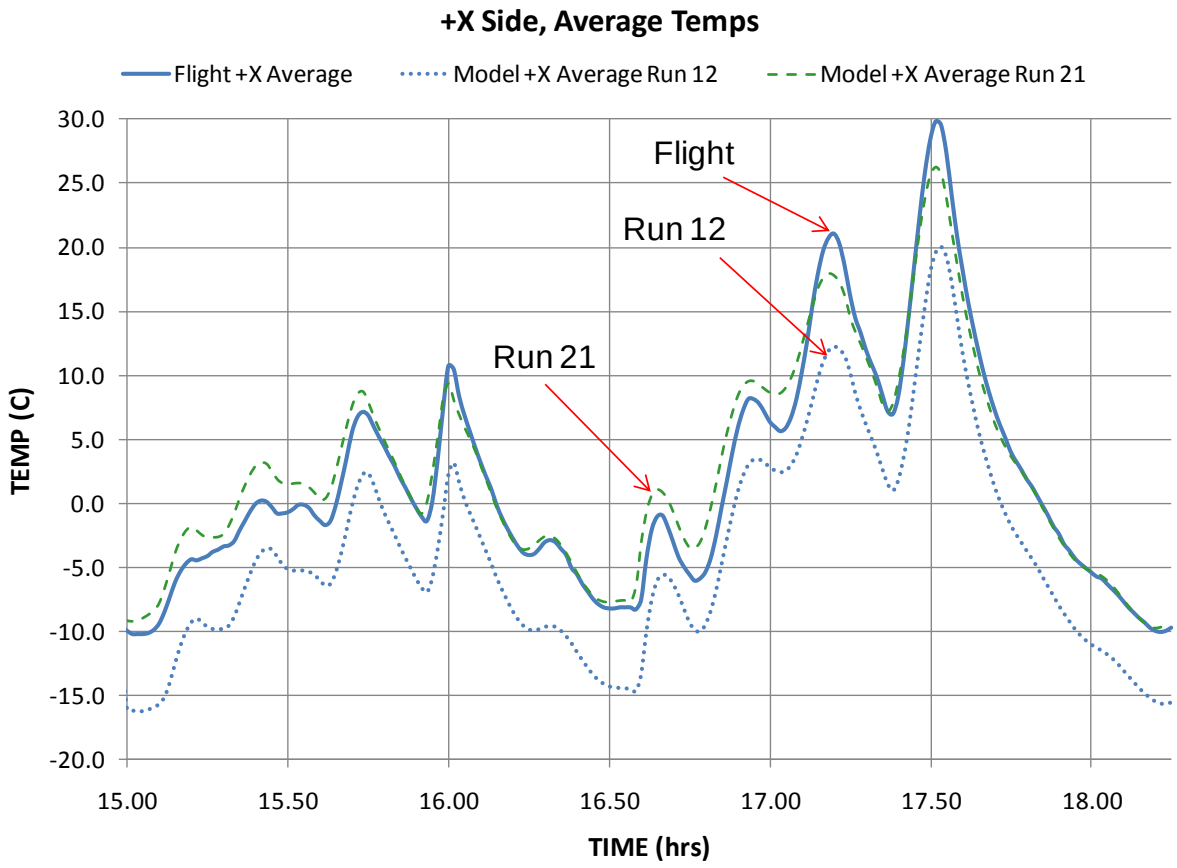

Figure 14. +X Side - Result from increased OLR value

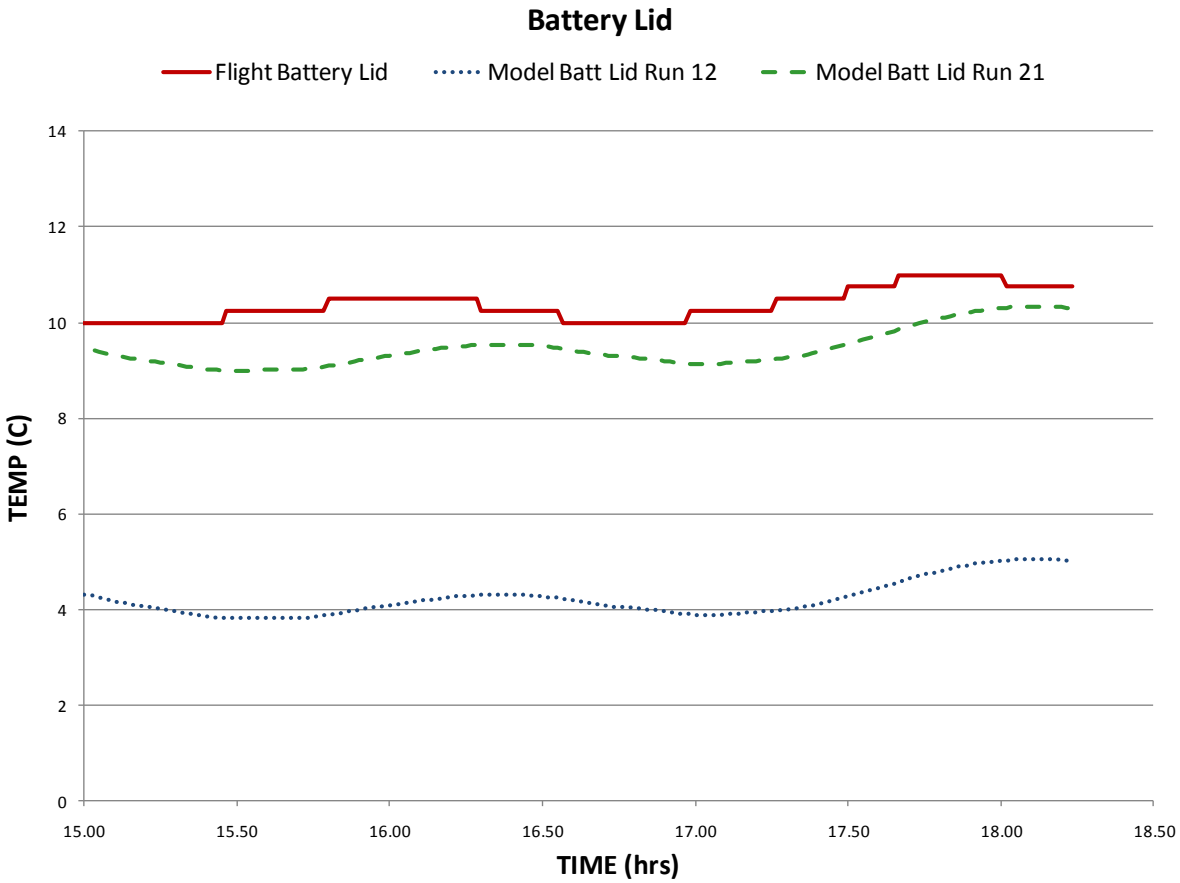

Figure 15. Battery Lid - Result from increased OLR value

Figures 16 and 17 display the +Y and +X sides comparisons of Run 12 versus Run 22. Run 12 is the baseline case with the mean albedo and OLR values of 0.27 and 211 W/m^2 respectively. Run 22 shows a case with the mean OLR value and a high albedo value of 0.40. The higher albedo values decreases the temperature gap between the flight data and model predictions. Once again, while it is possible for the albedo to be higher for this data set, there is no way to justify exactly what that value is for this period.

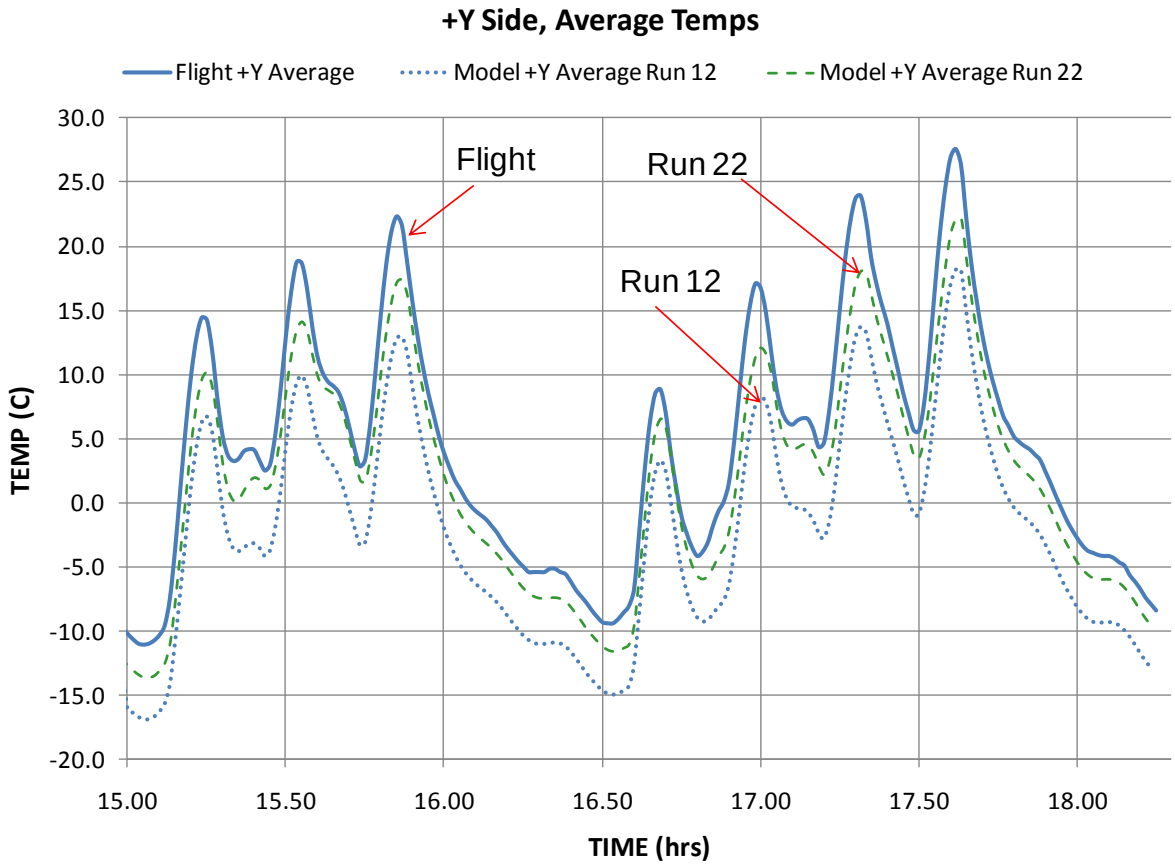

Figure 16. +Y Side - Result from increased albedo value

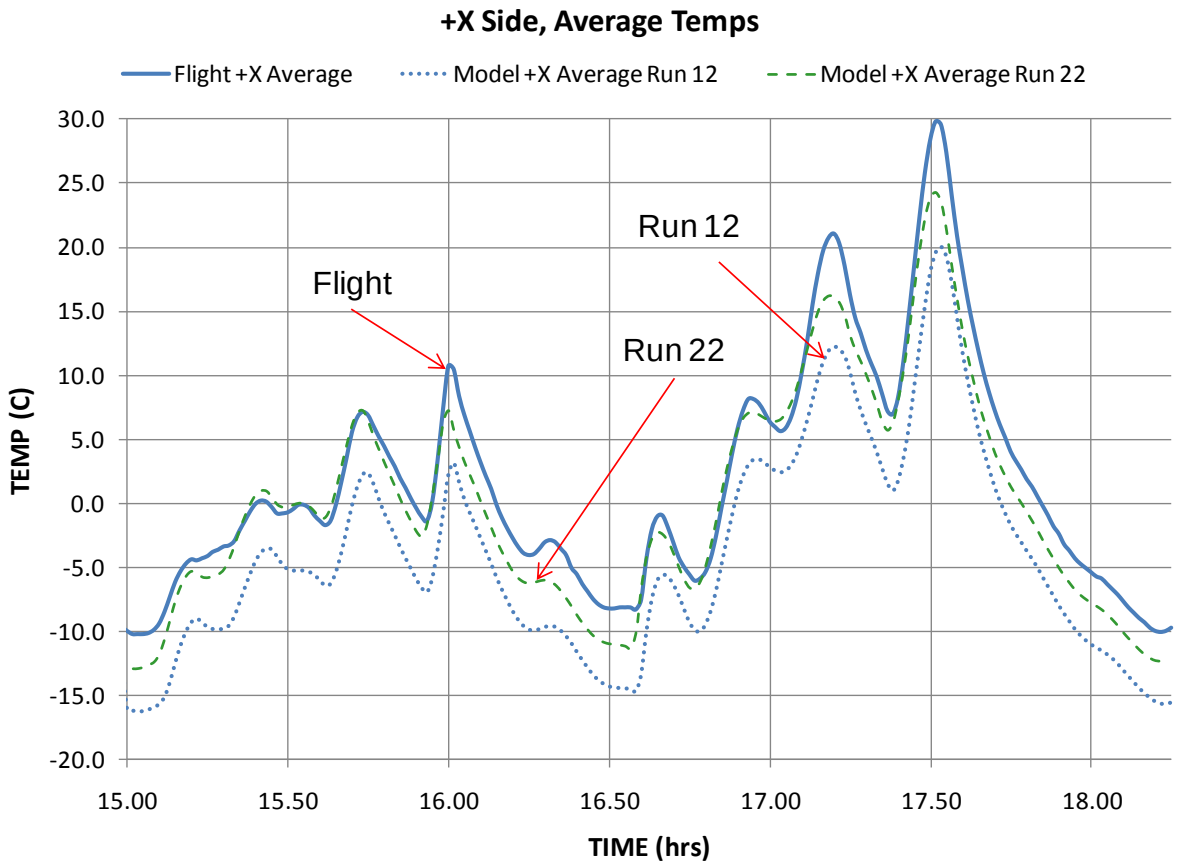

Figure 17. +X Side - Result from increased albedo value

The analysis predicted temperatures were always lower for first data set correlation. Since this data set was a cold case representation, it was determined that the design cold case environments from NASA-TM-2001-211221 are conservative and should continue to be utilized with the full application of the Kelly cosine factors on solar incident cell surfaces.

B. Data Set 2 Correlation Summary

Eleven cases were considered varying model parameters to understand the spacecraft's sensitivity to these changes. Appendix B summarizes the details of each case study. All model runs were performed on a high-end workstation. The total run time for the model using the second data set was approximately 33 hours. The largest portion of this was the heating rate calculations which averaged around 26 hours to complete. Internal radiation calculations were fulfilled in a little over 4 hours, while external radiation calculations could be accomplished in less than 1 hour. The final SINDA run took 1.5 hours to complete.

The ACS vector data was also supplied every second for this 48 hour data set. Using this much fidelity, would have resulted in 172,800 orbital positions. At roughly 2 minutes of run time per position, it would have taken approximately 240 days to run a single case for the second data set.

This type of precision was not necessary to obtain an accurate correlation. Therefore, a position was pulled once every 5 minutes over the 48 hour data set. This resulted in 576 positions. Based on the findings in the first data set, that proved to be a little too coarse for the two orbits use for the correlation. Consequently, positions were run at 5 minute intervals for orbits 1-23. Orbits 24 and 25 were run at 30 second intervals, and orbits 26-30 were run at 5 minute intervals. The flight temperature data was correlated to orbits 24 and 25 for the second data set.

Figures 18 and 19 show a comparison of increasing the orbital position fidelity from every 5 minutes to every 30 seconds for orbits 24 and 25. Figure 18 displays the average of all six solar clips on the +Y side, while Figure 19 shows the average of the six solar clips on the +X side. The solid blue line represents the flight temperature data. The dotted blue line displays the model temperatures from Run 1 which had an orbital position at 5 minute intervals. The solid green line represents Run 11 which had the increased fidelity to 30 second intervals for orbits 24 and 25. Both Figures 18 and 19 are using the design thermal math model with only minimal parameter updates. Those modifications were discussed in Section II of this paper and included changing the solar cell optical properties to reflect GaAs cells and a Sun angle dependent absorptivity. Nominal external environments were also applied and are detailed on the next page.

As shown in the following plots, increasing the position frequency provides little improvement over using the 5 minute position intervals. The satellite was more stable during this period and did not display the large temperature swings witnessed during the first data set. The 30 second position intervals during orbit 24 and 25 were kept throughout this second data set correlation effort to be consistent and because it did improve the correlation by a little over a 1°C.

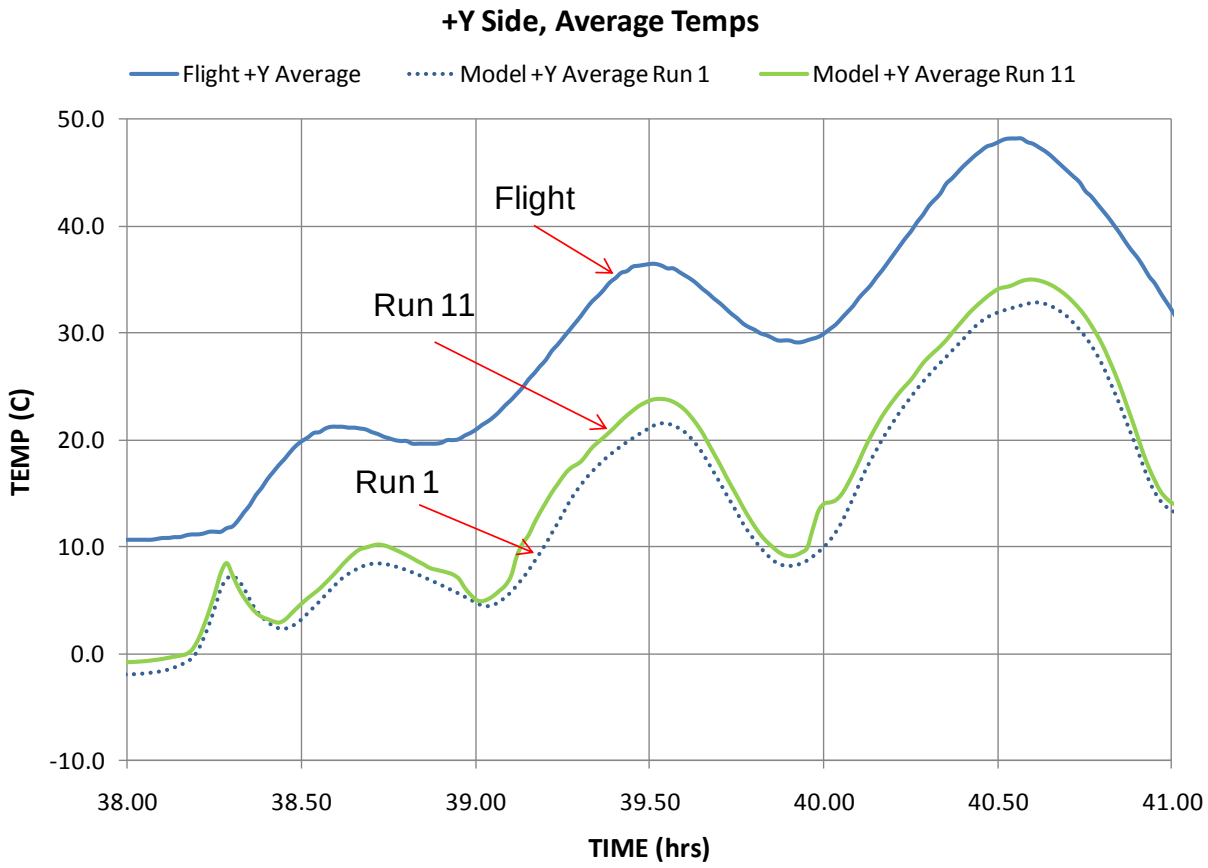

Figure 18. Data Set 2, +Y Side - Comparison of Orbital Position Frequency

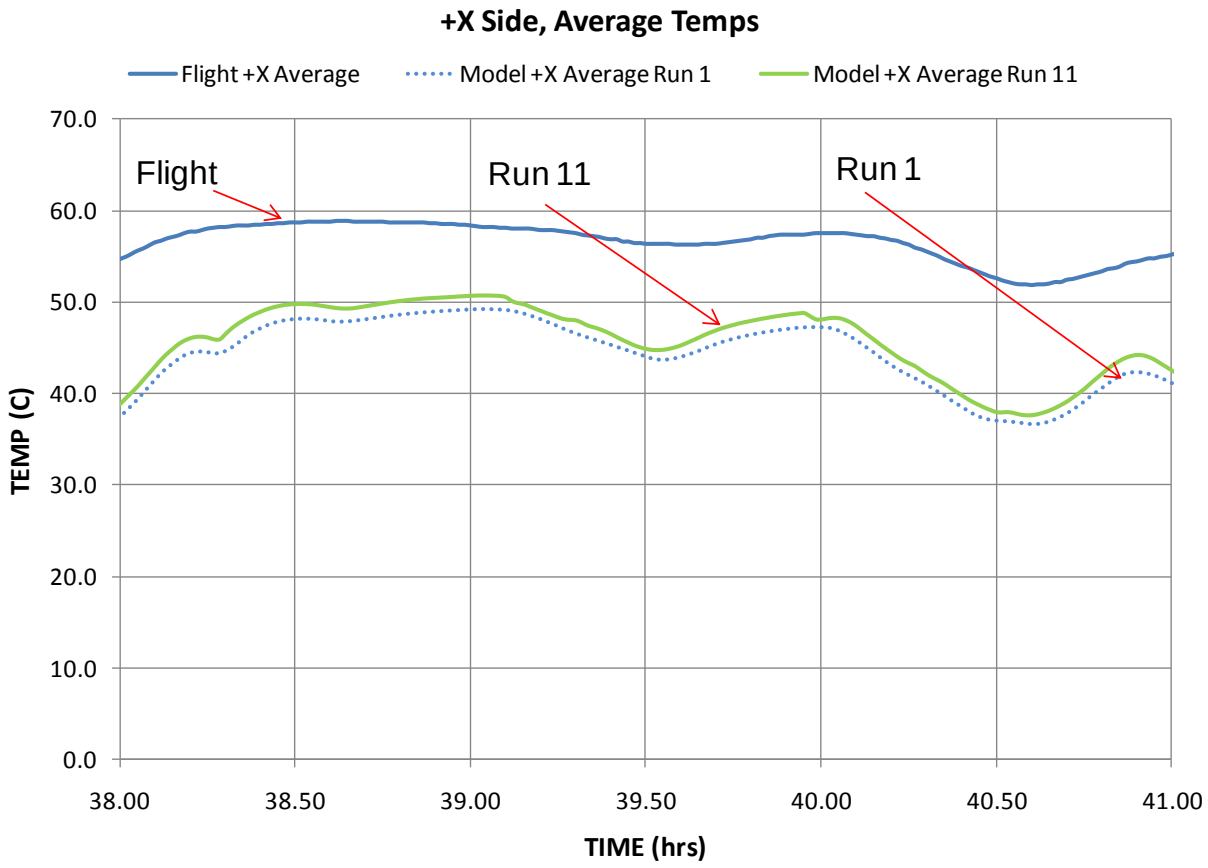

Figure 19. Data Set 2, +X Side - Comparison of Orbital Position Frequency

NASA/TM-2001-211221 was referenced to obtain the mean environments for high inclination orbits. A solar flux value of 1385 W/m^2 was calculated by scaling the median solar constant to the spacecraft's distance from the Sun on March 11-12, 2011. A mean albedo of 0.23 plus a 0.19 orbital average albedo correction factor was applied based on beta angle to give a total albedo value of 0.42. The mean OLR (Outgoing Longwave Radiation) for high inclination orbits of 211 W/m^2 was also applied. Figure 10 shows a table from NASA/TM-2001-211221 where the environments above were defined. The mean values that were used are enclosed in green. The minimum albedo and OLR values are enclosed in blue, while the maximum values are enclosed in red. This information is highlighted to show the range of external environments that is possible for this correlation. Figure 11 displays the albedo correction factor recommendations from NASA/TM-2001-211221. The correction factor of 0.19 was applied to the first data set to represent a beta angle of 75°.

As seen in Figures 18 and 19, the first few runs of the second data set correlation effort proved to be fairly agreeable. The model temperatures trend nicely with the rise and fall of the flight temperature data despite the few excursions mentioned previously regarding the loss of the spacecraft magnetometer and relying on an experiment's magnetometer. The model temperatures are running about 10-15°C cooler than the flight values. After reviewing the first set of runs, several model parameters were varied to better understand the spacecraft's sensitivity to these

parameter trades and close the temperature gap between the flight temperatures and the model predictions.

The vendor specifies a 25.1% solar cell efficiency. A case was run on the second data set lowering this value to 22% to account for on-orbit efficiency degradation. This was captured by calculating a new set of angle dependent absorptivity values using the lower efficiency values. Basically the absorptivity values were slightly higher at lower angles representing less energy being converted to power, meaning more energy would be dissipated as heat directly in the solar cells. This effect increased the model predicted temperatures by a couple of degrees.

The second data set occurs while the spacecraft is exposed to full Sun conditions. It is possible that the battery has reached a fully charged state and the sunlight absorbed in solar cells is being converted to heat in the panels.. A case was analyzed where the solar cell absorptivity was no longer corrected for power conversion but was set to a constant value of 0.925 for the full 48 hours (therefore basically saying the solar cells had an efficiency of 0%). Figures 20 and 21 display the results from varying this model parameter. Run 11 is the baseline case for the second data set, which includes no model changes except for those mentioned in Section II of this paper, adding the 30 second intervals during orbits 24 and 25, and applying nominal external environments as defined above. Run 10 represents applying a constant solar cell absorptivity of 0.925. As shown, this case significantly improved the correlation. It would take a vast amount of additional effort to sort through the power data and determine a time dependent solar cell efficiency for this 48 hour data set. Although, it appears to be part of the equation to obtaining a more accurate temperature correlation, this effort was not undertaken as part of this task.

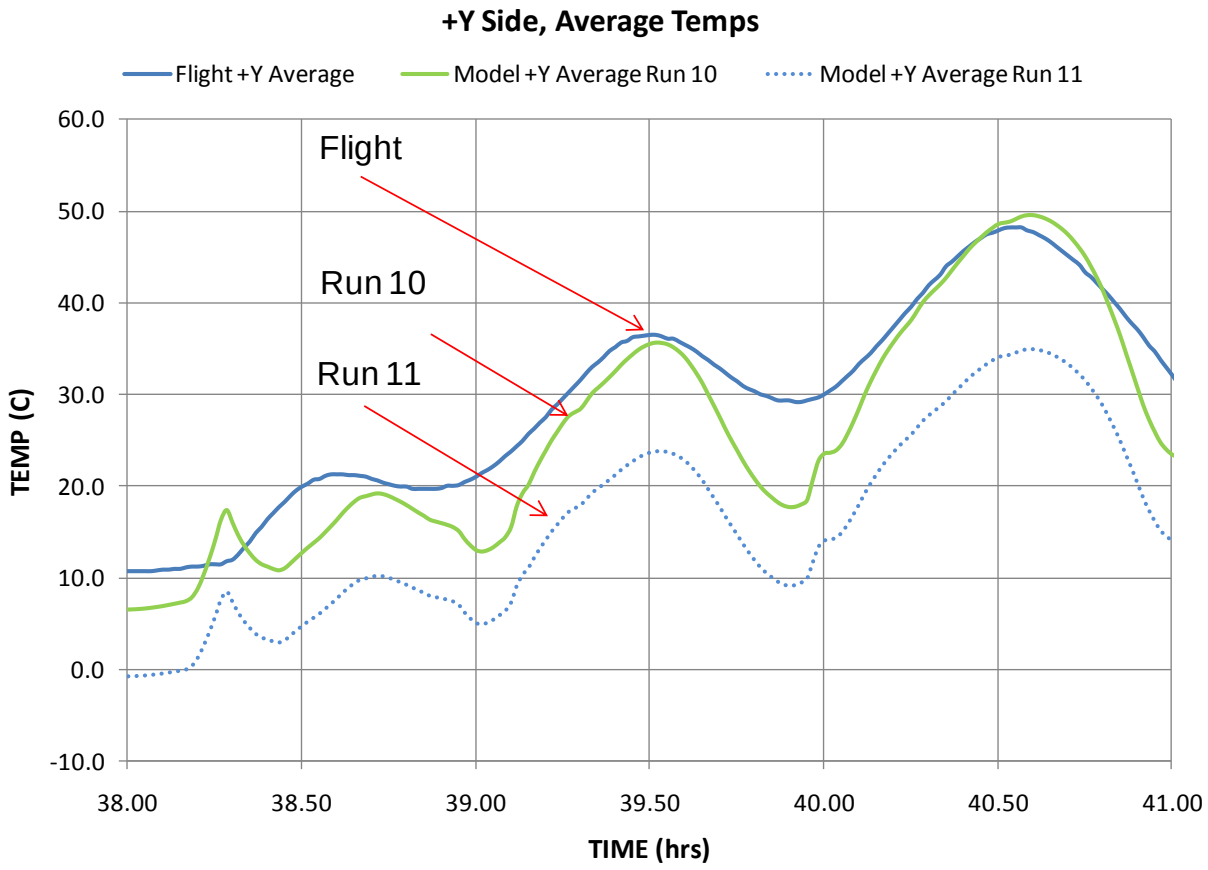

Figure 20. Data Set 2, +Y Side - Comparison of Decreased Solar Cell Efficiency

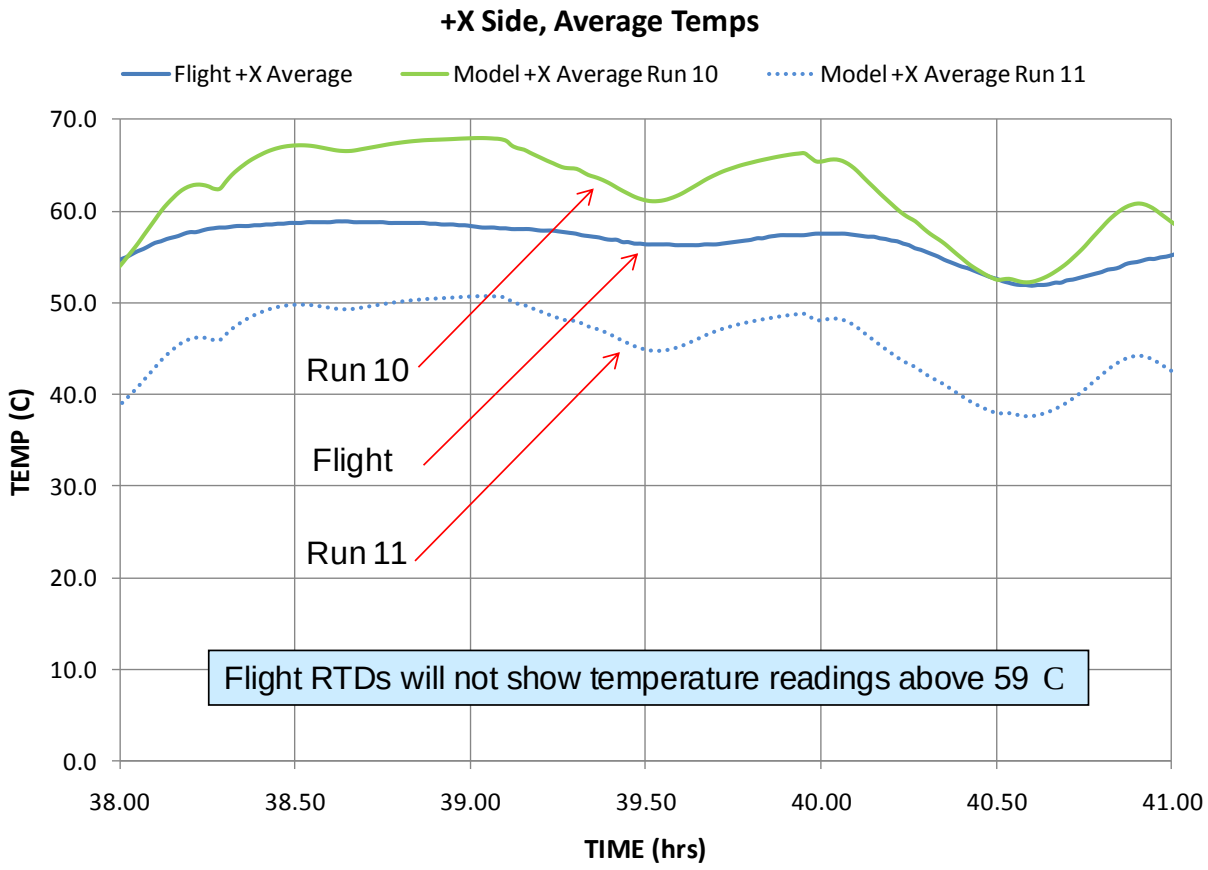

Figure 21. Data Set 2, +X Side - Comparison of Decreased Solar Cell Efficiency

The emissivity of the externally mounted solar cells was also considered for this data set. Cases were run with an emissivity value of 0.85 and 0.70. A similar outcome was noted as with the first data set. The model predicted temperatures respond largely to this parameter and the temperature correlation was very nice with an emissivity of 0.70. However, once the optical properties were tested on the spare solar clip, it proved the vendor data optical properties were the correct values to use.

As was the case in the low beta correlation attempt, modeling assumptions had very little effect on predicted temperatures. The temperature difference between flight data and analysis could also be caused by the difference between the assumed nominal external environment and the environment that was actually experienced during flight. The actual flight environment is probably some combination of higher albedo and OLR. As shown in Figure 10, 3σ values can be as high as 0.69 for albedo and 332 W/m^2 for OLR. While not likely that both values would be that high for a single orbit, one value could be high while the other might be somewhat average.

Multiple cases were considered using average albedo values with extreme OLR values, and then using an average OLR value with a higher albedo value. Figures 22 and 23 display the +Y and +X sides comparisons of Run 11 versus Run 8. Run 11 is the baseline case with the mean albedo and OLR values of 0.42 and 211 W/m^2 respectively. Run 8 shows a case with the mean albedo value of 0.42 and an extreme OLR value of 332 W/m^2 .

As noticed in Figures 22 and 23, the higher OLR value provides an improved correlation for the second data set. Once again, since there are no instruments on FASTSAT-HSV01 to measure the external environments of the spacecraft, there is no way of knowing the exact external environments during this 48 hour period.

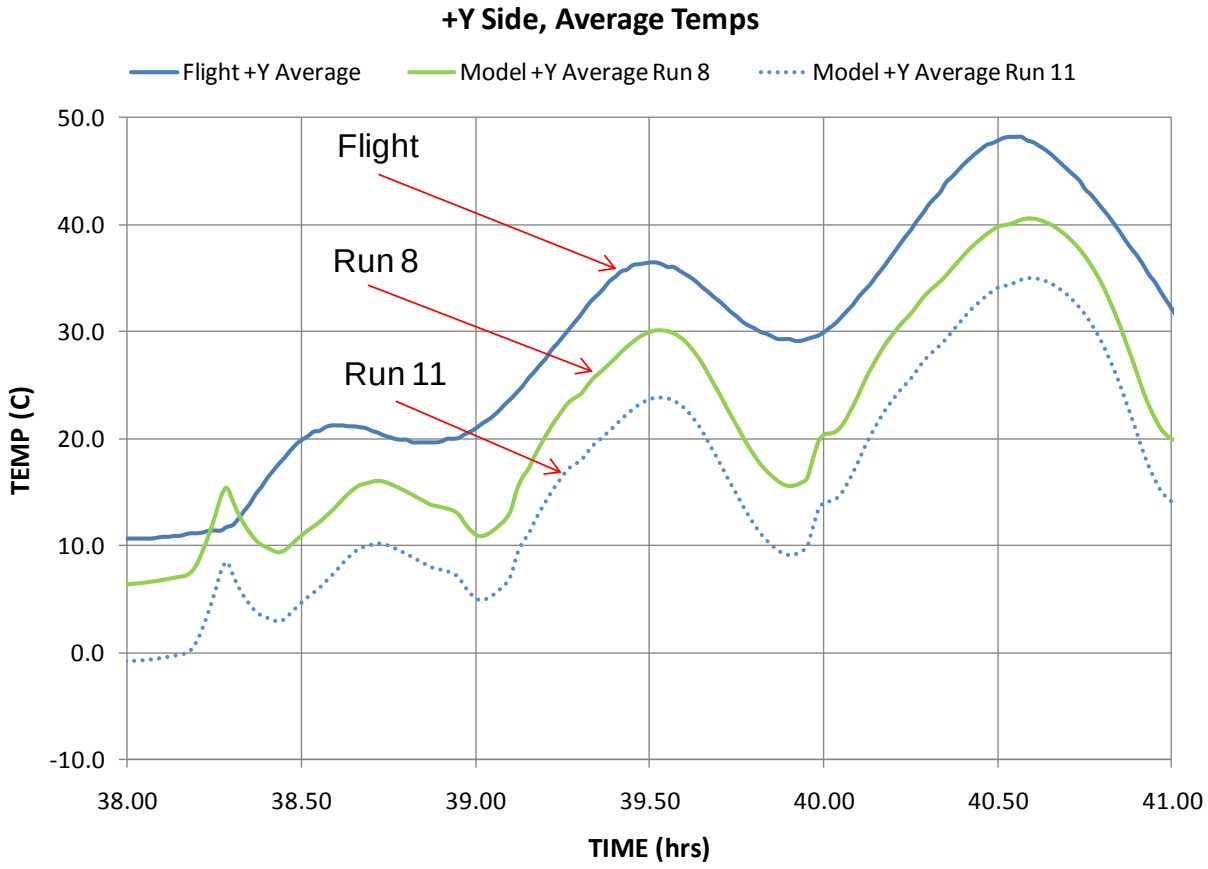

Figure 22. Data Set 2, +Y Side - Result from increased OLR value

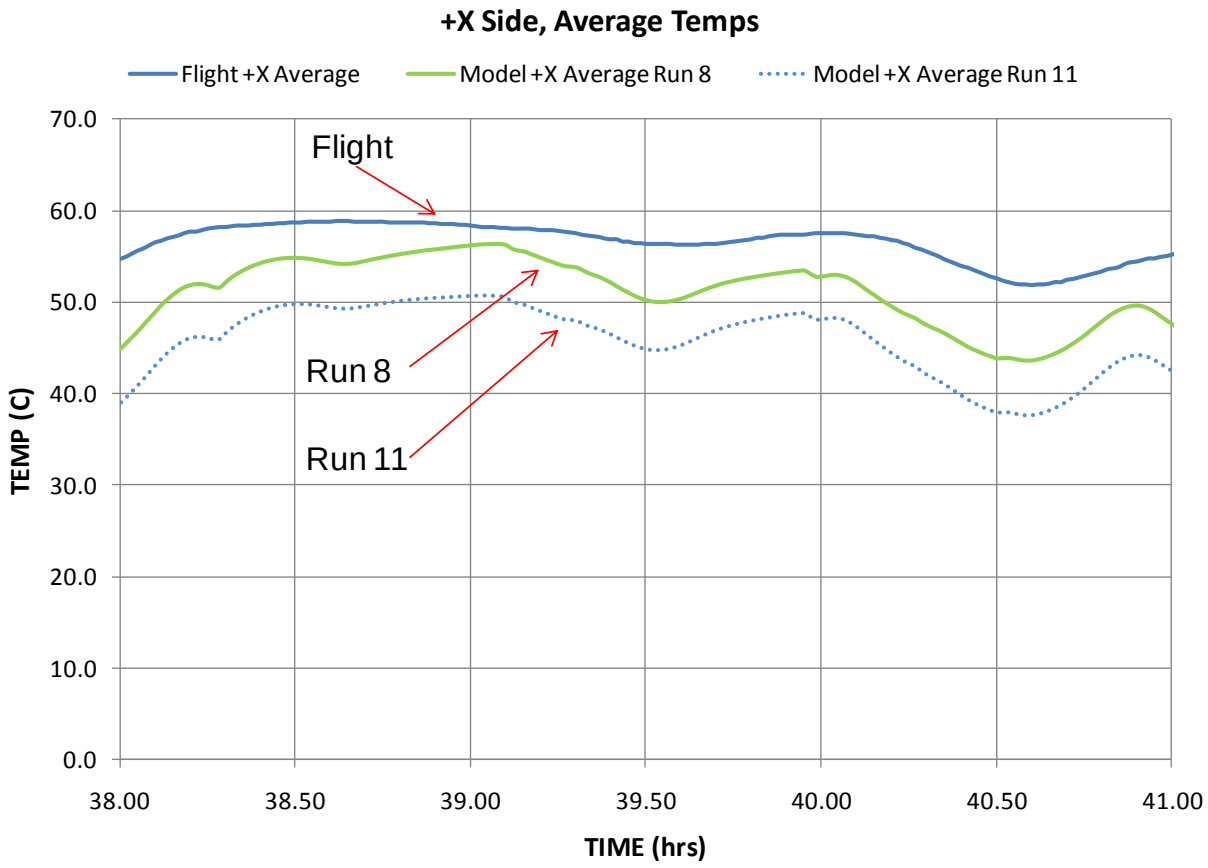

Figure 23. Data Set 2, +X Side - Result from increased OLR value

Based on the preceding cases, the actual environment was probably some combination of higher OLR and/or albedo than the mean values and increased internal heating in the solar cells due to fully charged battery effects. Additional cases could have been completed to determine if an exact combination of albedo and OLR could be found that matched the flight data, but realizing the model is within the variability of this unknown set of parameters is sufficient. It is recommended that the design hot case environments from NASA/TM-2001-211221 without accounting for power conversion within the solar cells be applied for any future design hot predictions.

V. Lessons Learned

There were many lessons learned during this correlation effort and these findings are listed below.

1.) The most obvious one is to conduct a thermal balance test and correlate the thermal model with the thermal balance test results. This will provide more confidence in the flight model due to being able to correlate to a known set of environments.

2.) If possible, measure all surface optical properties during the design phase. Coatings can vary from batch to batch and measured values will provide the most accuracy in the thermal model.

3.) Use worst case external environments for the hot and cold case temperature predictions. (which is typically standard practice for most aerospace companies). This would include applying the albedo correction factors and ignoring solar cell power conversion for worst case hot considerations.

4.) Obtain realistic component heat dissipation rates, especially for the power conversion components such as solar cells, battery, battery charge regulators and power distribution boxes. This will provide more accurate temperature predictions during the design phase. This would also allow for a more confident correlation of internal electronics boxes to flight temperature data.

5.) Expand the temperature range for the RTDs. Find the right balance between temperature range and resolution so that all flight temperatures are captured accurately during the mission.

Acknowledgements

The author would like to extend great appreciation to Ken Kittredge of MSFC, thermal lead for the FASTSAT-HSV01 project. Ken provided a significant amount of guidance during this effort. The author would also like to acknowledge John Sharp, Greg Schunk, and Shawn Breeding of MSFC for their feedback regarding this task.

Acronyms

ACS	Attitude Control System
DoD	Department of Defense
FASTSAT-HSV01	Fast Affordable Science and Technology SATellite-Huntsville
MSFC	Marshall Space Flight Center
NASA	National Aeronautics and Space Administration
PPOD	Poly Picosatellite Orbital Deployer
RTD	Resistance Temperature Device

Appendix A

(The significant cases that were discussed in this paper are highlighted.)

Data Set 1: February 6, 2011 - 18 hour period around Beta 0°								
Run	**Albedo**	**Earth IR (W/m^2)**	**Frequency of Orbit Position for last 2 orbits**	**Solar Cell Emissivity**	**Solar Cell Efficiency**	**Contactor Conductance Value between panels and structure ($BTU/hr/in^2/°F$)**	**Contactor Conductance between panels and solar clips**	**Other**
1	0.27	211	5 min	0.85	25.1%	1.2	0.065 inches of Tedlar	
2	0.27	211	5 min	0.85	25.1%	0	0.065 inches of Tedlar	
3	0.27	211	5 min	0.85	25.1%	0.6	0.065 inches of Tedlar	
4	0.27	211	5 min	0.85	25.1%	0.3	0.065 inches of Tedlar	
5	0.27	211	5 min	0.85	25.1%	1.2	0.065 inches of Tedlar	Black anodized internal coating emissivity changed to 0.82 instead of 0.90
6	0.27	211	5 min	0.85	25.1%	1.2	0.01 inches of Tedlar	
7	0.27	211	5 min	0.85	25.1%	1.2	0.065 inches of G10	

Data Set 1: February 6, 2011 - 18 hour period around Beta 0° (continued)								
8	0.27	211	5 min	0.85	25.1%	1.2	0. 5 inches of G10	
9	0.27	211	30 sec	0.80	25.1%	1.2	0.065 inches of Tedlar	
10	0.27	211	30 sec	0.80	25.1%	2.4	0.065 inches of Tedlar	
11	0.27	211	30 sec	0.80	25.1%	50	0.065 inches of Tedlar	
12	0.27	211	30 sec	0.85	25.1%	1.2	0.065 inches of Tedlar	BASELINE CASE for Data Set 1
13	0.27	211	30 sec	0.85	25.1%	0.3	0.065 inches of Tedlar	
14	0.27	211	30 sec	0.80	25.1%	0	0.065 inches of Tedlar	
15	0.27	211	30 sec	0.80	25.1%	0.2	0.065 inches of Tedlar	
16	0.27	211	30 sec	0.85	25.1%	1.2	0.065 inches of Tedlar	Energy balance & max temp from 0.01 to 0.001
17	0.27	211	30 sec	0.70	25.1%	1.2	0.065 inches of Tedlar	
18	0.27	211	30 sec	0.70	25.1%	12	0.065 inches of Tedlar	

Data Set 1: February 6, 2011 - 18 hour period around Beta 0° (continued)								
19	0.27	244	30 sec	0.83	25.1%	1.2	0.065 inches of Tedlar	Began using measured solar cell optical properties
20	0.27	218	30 sec	0.83	25.1%	1.2	0.065 inches of Tedlar	
21	0.27	300	30 sec	0.83	25.1%	1.2	0.065 inches of Tedlar	Increased Earth IR value
22	0.40	211	30 sec	0.83	25.1%	1.2	0.065 inches of Tedlar	Increased Albedo value
23	0.27	211	30 sec	0.83	25.1%	1.2	0.065 inches of Tedlar	
24	0.27	211	30 sec	0.83	25.1%	0	0.065 inches of Tedlar	Isolated solar cells
25	0.27	211	30 sec	0.83	25.1%	12	0.065 inches of Tedlar	
26	0.27	211	30 sec	0.83	25.1%	1.2	0.5 inches of Tedlar	
27	0.27	211	30 sec	0.83	25.1%	1.2	0 inches of Tedlar	
28	0.27	211	30 sec	0.83	25.1%	1.2	0.0325 inches of Tedlar	

Appendix B

(The significant cases that were discussed in this paper are highlighted.)

Data Set 2: March 11-12, 2011 - 48 hour period around Beta 75°								
Run	**Albedo**	**Earth IR (W/m^2)**	**Frequency of Orbit Position for last 2 orbits**	**Solar Cell Emissivity**	**Solar Cell Efficiency**	**Contactor Conductance Value between panels and structure ($BTU/hr/in^2/°F$)**	**Contactor Conductance between panels and solar clips**	**Other**
1	0.42	211	5 min	0.85	25.1%	1.2	0.065 inches of Tedlar	
2	0.42	211	5 min	0.70	25.1%	1.2	0.065 inches of Tedlar	
3	0.42	211	30 sec	0.70	25.1%	1.2	0.065 inches of Tedlar	
4	0.42	211	30 sec	0.70	25.1%	12	0.065 inches of Tedlar	
5	0.42	211	30 sec	0.70	0%	12	0.065 inches of Tedlar	Solar cell absorptivity kept at constant value of 0.925
6	0.42	211	30 sec	0.70	22%	1.2	0.01 inches of Tedlar	
7	0.42	300	30 sec	0.83	25.1%	1.2	0.065 inches of Tedlar	Began using measured solar cell optical properties

Data Set 2: March 11-12, 2011 - 48 hour period around Beta 75° (continued)								
8	0.42	332	30 sec	0.83	25.1%	1.2	0.065 inches of Tedlar	Increased Earth IR value
9	0.42	300	30 sec	0.83	0%	1.2	0.065 inches of Tedlar	Solar cell absorptivity kept at constant value of 0.925
10	0.42	211	30 sec	0.83	0%	1.2	0.065 inches of Tedlar	Solar cell absorptivity kept at constant value of 0.925
11	0.42	211	30 sec	0.83	25.1%	1.2	0.065 inches of Tedlar	BASELINE CASE for Data Set 2